# Slant Wire Models Using Accurate Correction Techniques in FDTD Method

Kazuo Yamamoto [1] and Hiroyuki Iki [2]

(1) Dept. of Control Engineering, Nara National College of Technology, Yamato-Koriyama, Nara, 639-1080, Japan (e-mail: kazuo@ctrl.nara-k.ac.jp), (2) FFC Systems Limited, Shinjuku Koyama Bldg., 4-30-3, Yoyogi, Shibuya, Tokyo, 151-0053, Japan (e-mail: iki-h@ffc.co.jp).

***Abstract* – This paper presents a simple slant wire model for lightning surge analyses using accurate correction techniques to decrease error caused by a numerical difference used around a slant wire in FDTD method.**

**The proposed method is to apply an implicit scheme around a diagonal wire, and turn the first order finite difference into the second order. The numerical formulation of the proposed method is explained, and the comparison between slant wire models and a measured result for real applications is shown.**

***Keywords*** – Slant Wire, FDTD Method, Surge Analysis, Implicit Scheme, Maxwell's Equation

## I. INTRODUCTION

Very fast surge phenomena in a three dimensional structure, which includes surge propagation in a transmission tower and in a tall building, can not be simulated by an existing surge simulator such as EMTP and ATP [1] accurately, because the distributed-parameter circuit theory in those simulators assumes the plane-wave propagation. Therefore, such simulations are aboundingly carried out by using the FDTD ( Finite-Difference Time-Domain ) method in these days [2,3]. The FDTD method has been applied to many cases of antenna analyses [4] and has been yielded many good results. However, the method has not been applied to power system simulations very much because of enormous storage capacity and huge calculation time. In these days, those problems about computing power are in the process of being solved, some FDTD applications to the part of a power system are introduced [5,6].

The FDTD method is based on Maxwell's equations. Maxwell's equations consist of Faraday's and Ampere's laws which mean electric and magnetic rotations respectively, those lows are discriminated in time dimension and in 3-D space. Behavior of electromagnetic fields is analyzed numerically according to information from geometric arrangements and shape of objects, and electric features such as conductivity, permittivity and permeability. When the FDTD method is applied for surge simulations of power systems, there are some problems. One of those problems is that a slant wire not existing on a grid can not be modeled correctly because the analysis space is broken up into cuboidal FDTD cells. To solve these problems, Subcell method [3] and other methods [7- 9] are proposed. However, the propagation time and so on have comparatively big error when the existing slant wire model is used for a surge simulation.

This paper presents slant wires correctly modeled by means of an implicit scheme for a FDTD surge simulation, and the proposed method turns the first order finite difference into the second order. The proposed method makes it possible to model arbitrary slant wires which are parallel to one of the possible three planes of the grids composing a FDTD cell. When the magnetic fields, whose direction is perpendicular against the direction of the slant wire and which are located around the slant wire, are calculated, the path of the rotating integration around the slant wire is changed to the path including the slant wire. The electric fields, which are located on the grids passing the slant wire, are compensated by an adjacent electric field. Furthermore, the magnetic fields located on the center of the surface which is vertical against the surface including the slant wire are recalculated. To evaluate the proposed method, the calculation results with the proposed method are compared with the measured result[10] and the calculated result with a wire model on FDTD grids.

In this paper, A self-produced FDTD program [11] developed for general purpose surge simulation using the FDTD method is used.

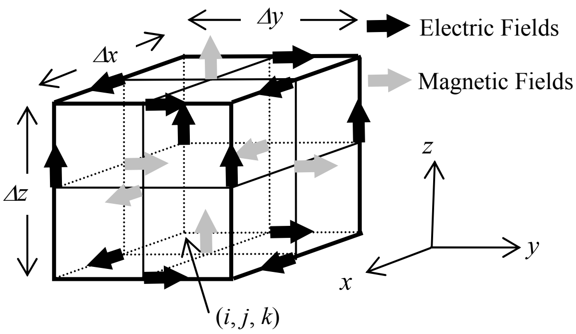


Fig.1 Configuration of electric and magnetic fields in a cell

## II. FDTD EQUATIONS

Differential forms of Maxwell's equations to formulate the FDTD equations can be shown as follows.

$$\mathrm{rot}\mathbf{H}(\mathbf{r},t)=\frac{\partial \mathbf{D}(\mathbf{r},t)}{\partial t}+\mathbf{J}(\mathbf{r},t) \tag{1}$$

$$\mathrm{rot}\mathbf{E}(\mathbf{r},t)=-\frac{\partial \mathbf{B}(\mathbf{r},t)}{\partial t} \tag{2}$$

where : **E** [V/m] is a vector of electrical field, **H** [A/m] is a vector of magnetic field, **D** [C/m$^2$] is a vector of electric flux density, **B** [T] is a vector of magnetic flux density and

**J** [A/m$^2$] is current density. (1) shows Ampere's law and (2) shows Faraday's law of electromagnetic induction.

Yee's algorithm [2, 3] is applied to (1) and (2) to differentiate centrally on time dimension and on the 3-D cell shown in Fig. 1. The formulas of the fundamental FDTD method can be derived as follows.

$$E_x^n\left(i+\frac{1}{2},j,k\right) = K_{1x}\left(i+\frac{1}{2},j,k\right)E_x^{n-1}\left(i+\frac{1}{2},j,k\right) + K_{2x}\left(i+\frac{1}{2},j,k\right) \times \frac{1}{\Delta z \Delta y}\left\{\left[H_z^{n-\frac{1}{2}}\left(i+\frac{1}{2},j+\frac{1}{2},k\right) - H_z^{n-\frac{1}{2}}\left(i+\frac{1}{2},j-\frac{1}{2},k\right)\right]\Delta z - \left[H_y^{n-\frac{1}{2}}\left(i+\frac{1}{2},j,k+\frac{1}{2}\right) - H_y^{n-\frac{1}{2}}\left(i+\frac{1}{2},j,k-\frac{1}{2}\right)\right]\Delta y\right\} \quad (3)$$

$$H_x^{n+\frac{1}{2}}\left(i,j+\frac{1}{2},k+\frac{1}{2}\right) = H_x^{n-\frac{1}{2}}\left(i,j+\frac{1}{2},k+\frac{1}{2}\right) - K_{3x}\left(i,j+\frac{1}{2},k+\frac{1}{2}\right) \times \frac{1}{\Delta z \Delta y}\left\{\left[E_z^n\left(i,j+1,k+\frac{1}{2}\right) - E_z^n\left(i,j,k+\frac{1}{2}\right)\right]\Delta z - \left[E_y^n\left(i,j+\frac{1}{2},k+1\right) - E_y^n\left(i,j+\frac{1}{2},k\right)\right]\Delta y\right\} \quad (4)$$

$$K_{1x}\left(i+\frac{1}{2},j,k\right) = \frac{1-\dfrac{\sigma\left(i+\frac{1}{2},j,k\right)\Delta t}{2\varepsilon\left(i+\frac{1}{2},j,k\right)}}{1+\dfrac{\sigma\left(i+\frac{1}{2},j,k\right)\Delta t}{2\varepsilon\left(i+\frac{1}{2},j,k\right)}} \quad (5)$$

$$K_{2x}\left(i+\frac{1}{2},j,k\right) = \frac{\dfrac{\Delta t}{\varepsilon\left(i+\frac{1}{2},j,k\right)}}{1+\dfrac{\sigma\left(i+\frac{1}{2},j,k\right)\Delta t}{2\varepsilon\left(i+\frac{1}{2},j,k\right)}} \quad (6)$$

$$K_{3x}\left(i,j+\frac{1}{2},k+\frac{1}{2}\right) = \frac{\Delta t}{\mu\left(i,j+\frac{1}{2},k+\frac{1}{2}\right)} \quad (7)$$

where : $\mu$ is permeability, $\varepsilon$ is permittivity, $\rho$ is conductivity. Electric and magnetic fields to x direction have been shown as above, the one to y and z directions can be derived similarly as (3) to (7). The electric and magnetic fields are calculated alternately at intervals of $\Delta t/2$ where $\Delta t$ is a discrete time interval.

## III. Simplified Slant Wire Models

The proposed method makes it possible to express a slant wire on an arbitrary surface composing a FDTD cell shown in Fig. 1. In this case, two types of slant wire shown in Fig. 2 (a) and (b) can be thought of. Fig. 2 (a) shows that a slant wire goes across a grid to the opposite grid, and Fig. 2 (b) shows that a slant wire goes across a grid to the adjacent grid. Two electric fields on the grid where a slant wire goes across are allocated on both hands of intersections between the slant wire and grids, such as

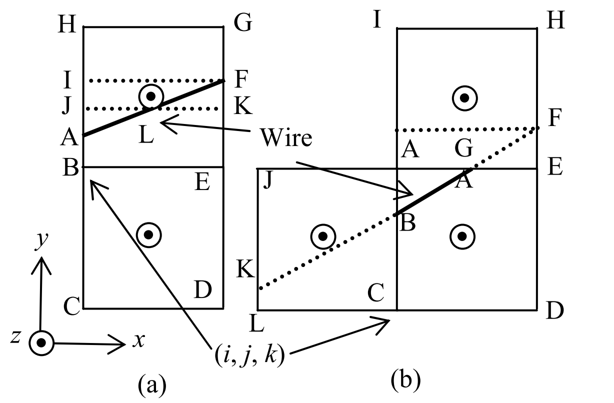


Fig.2 Configuration of a diagonal wire

electrical fields on grids AB, AH, EF and FG in Fig. 2 (a), and electrical fields on grids AB, BC, EG, AG in Fig. 2 (b). When the magnetic fields adjacent to the slant wire such as $H_z(i+1/2, j+1/2, k)$ and $H_z(i+1/2, j-1/2, k)$ in Fig. 2 (a), and $H_z(i+1/2, j+1/2, k)$ and $H_z(i+1/2, j+3/2, k)$ in Fig. 2 (b) are calculated, the common paths of integration BCDEB in Fig. 2(a) and ACDEA in Fig. 2(b) are changed to the path including the slant wire such as ABCDEFA in Fig. 2 (a) and BCDEFB in Fig 2 (b) respectively.

In a simplified slant wire model, electric fields on the grids which the slant wire goes across are approximated by adjacent electrical fields in the parallel direction with the approximated electrical fields. In a common FDTD method, one electric field is allocated on one grid, however, two hypothetical electric fields are allocated on one grid which the slant wire goes across to model the slant wire as above.

In the example shown in Fig. 2 (a), we give a full detail of above theories as following. Newly allocated electric fields are as follows.

$$E_y\left(i,j+\frac{AB}{2\Delta y},k\right) = E_y\left(i,j-\frac{1}{2},k\right), \quad E_y\left(i,j+1-\frac{AH}{2\Delta y},k\right) = E_y\left(i,j+\frac{3}{2},k\right) \quad (8)$$

$$E_y\left(i+1,j+\frac{EF}{2\Delta y},k\right) = E_y\left(i+1,j-\frac{1}{2},k\right), \quad E_y\left(i+1,j+1-\frac{FG}{2\Delta y},k\right) = E_y\left(i+1,j+\frac{3}{2},k\right) \quad (9)$$

Electric fields adjacent to the slant wire apart from (8) and (9) are calculated. As the magnetic field $H_z(i+1/2, j-1/2, k)$ calculated along the path ABCDEFA of integration is equivalent of the one calculated along the path BCDEB, $E_x(i+1/2, j, k)$ which is an electrical field on BE can be calculated from the following equation.

$$E_x\left(i+\frac{1}{2},j,k\right) = E_y\left(i,j-\frac{1}{2},k\right)\cdot\frac{AB}{\Delta x} - E_y\left(i+1,j-\frac{1}{2},k\right)\cdot\frac{EF}{\Delta x} \quad (10)$$

It should be noted that the above simplified slant wire model has been derived by use of an approximation that the flux penetrating ABEFA is zero. This approximation make the slant model in FDTD method stable, but the model has comparatively large error.

The magnetic field $H_z(i+1/2, j-1/2, k)$ is calculated along the path ABCDEFA of integration similarly as the derivation of (10).

$$H_z^{n+\frac{1}{2}}\left(i+\frac{1}{2},j-\frac{1}{2},k\right)=H_z^{n-\frac{1}{2}}\left(i+\frac{1}{2},j-\frac{1}{2},k\right) \quad (11)$$
$$-K_{3z}\left(i+\frac{1}{2},j-\frac{1}{2},k\right)\frac{1}{\Delta y\Delta x}\left\{E_x^n\left(i+\frac{1}{2},j-1,k\right)\Delta x\right.$$
$$\left.+E_y^n\left(i+1,j-\frac{1}{2},k\right)\left(1+\frac{EF}{\Delta y}\right)\Delta y-E_y^n\left(i,j-\frac{1}{2},k\right)\left(1+\frac{AB}{\Delta y}\right)\Delta y\right\}$$

$H_z$( $i$+1/2, $j$-1/2, $k$ ) is also calculated along the path AFGHA of integration.

The magnetic field $H_x$( $i$, $j$+1/2, $k$+1/2 ) on the surface which is vertical to the surface including the slant wire is calculated from $E_y$( $i$, $j$+AB/2Δ$y$, $k$ ) and $E_y$( $i$, $j$+1-AH/2Δ$y$, $k$ ) which have already been recalculated in (8) and (9) respectively.

$$H_x^{n+\frac{1}{2}}\left(i,j+\frac{1}{2},k+\frac{1}{2}\right)=H_x^{n-\frac{1}{2}}\left(i,j+\frac{1}{2},k+\frac{1}{2}\right)-K_{3x}\left(i,j+\frac{1}{2},k+\frac{1}{2}\right)$$
$$\times\left\{\left[E_z^n\left(i,j+1,k+\frac{1}{2}\right)-E_z^n\left(i,j,k+\frac{1}{2}\right)\right]\Delta z-E_y^n\left(i,j+\frac{1}{2},k+1\right)\Delta y\right.$$
$$\left.+E_y^n\left(i,j-\frac{1}{2},k\right)AB+E_y^n\left(i,j+\frac{3}{2},k\right)AH\right\}\times\frac{1}{\Delta z\Delta y} \quad (12)$$

$H_x$( $i$, $j$+1/2, $k$-1/2 ), $H_x$( $i$+1, $j$+1/2, $k$-1/2 ) and $H_x$( $i$+1, $j$+1/2, $k$-1/2 ) can also be calculated similarly as $H_x$( $i$, $j$+1/2, $k$+1/2 ) in (12).

This simplified slant wire model has some advantages and disadvantages. If above (8) to (12) are used to model a slant wire, the flux penetrating the surface ABEF is zero. Therefore, such approximation becomes one of the sources of error even though the magnitude of error depends on the area of ABEF. Only truncation error of over second order arises from the rotating integration along the path of BCDEB in Fig. 2 (a) to model wire on FDTD grids. However, the $y$ directional difference of $E_x$ causes truncation error of first order when $H_z$( $i$+1/2, $j$-1/2, $k$ ) of (11) is calculated along the path of ABCDEFA in Fig. 2 (a) to model the simplified slant wire. The advantage of this simplified slant wire model is good numerical stability when a lot of slant wire are used in a FDTD simulation space. The detail slant model is proposed in the next chapter to solve those problems.

## IV. Detailed Slant Wire Model with Implicit Scheme

The proposed detailed slant wire model is explained here according to Fig. 2 (a). When the segment AF is a conductor, the magnetic flux penetrating the triangle JAL is equal to the amount of the magnetic flux penetrating the triangle KFL, but each magnetic flux is in the opposite direction. To represent conductor AF in the analysis space, an assumption that $H_z$( $i$+1/2, $j$-1/2, $k$ ) calculated from the path ABCDEFA of integration is equivalent to that calculated from the path ABCDEKJA of integration.

The following magnetic field $H_z$( $i$+1/2, $j$-1/2, $k$ ) is derived from applying Faraday's law to BCDE.

$$H_z^{n+\frac{1}{2}}\left(i+\frac{1}{2},j-\frac{1}{2},k\right)=H_z^{n-\frac{1}{2}}\left(i+\frac{1}{2},j-\frac{1}{2},k\right)-K_{3z}\left(i+\frac{1}{2},j-\frac{1}{2},k\right)$$
$$\times\frac{1}{\Delta x\Delta y}\left\{\left[E_y^n\left(i+1,j-\frac{1}{2},k\right)-E_y^n\left(i,j-\frac{1}{2},k\right)\right]\Delta y\right.$$
$$\left.-\left[E_x^n\left(i+\frac{1}{2},j,k\right)-E_x^n\left(i+\frac{1}{2},j-1,k\right)\right]\Delta x\right\} \quad (13)$$

The second term of right side member fulfills the following condition.

$$-K_{3z}\times\frac{1}{(\text{Area of BCDE})}\times\{\text{Circuital Integration of }\mathbf{E}\text{ on BCDE}\}$$

As $H_z$( $i$+1/2, $j$-1/2, $k$ ) calculated from the path of ABCDEFA is equivalent to that of the path of ABCDEKJA, the following (14) can be derived from Faraday's law by means of the central difference of $\partial E_x/\partial y$ and $\partial E_y/\partial x$. The magnitude of $E_x$ on KL is equivalent to that of $E_x$ on KJ, and each electric field is in the opposite direction. Therefore, the integration of $E_y$ on JA is equivalent of that of $E_y$ on KF.

$$H_z^{n+\frac{1}{2}}\left(i+\frac{1}{2},j-\frac{1}{2},k\right)=H_z^{n-\frac{1}{2}}\left(i+\frac{1}{2},j-\frac{1}{2},k\right)-K_{3z}\left(i+\frac{1}{2},j-\frac{1}{2},k\right)$$
$$\times\frac{1}{\Delta x\Delta y\left(1+\frac{EK}{\Delta y}\right)}\left\{E_x^n\left(i+\frac{1}{2},j-1,k\right)\Delta x\right. \quad (14)$$
$$\left.+E_y^n\left(i+1,j-\frac{1}{2},k\right)\left(1+\frac{EF}{\Delta y}\right)\Delta y-E_y^n\left(i,j-\frac{1}{2},k\right)\left(1+\frac{AB}{\Delta y}\right)\Delta y\right\}$$

From above (13) and (14), $E_x$( $i$+1/2, $j$, $k$ ) can be derived as follows.

$$E_x^n\left(i+\frac{1}{2},j,k\right)=\left\{\left(\frac{EK}{\Delta y}\right)E_x^n\left(i+\frac{1}{2},j-1,k\right)\Delta x\right.$$
$$\left.-\left(\frac{KF}{\Delta y}\right)\Delta y\left[E_y^n\left(i+1,j-\frac{1}{2},k\right)+E_y^n\left(i,j-\frac{1}{2},k\right)\right]\right\}\frac{1}{(1+EK/\Delta y)\Delta x} \quad (15)$$

When (14) was derived, the central difference in time dimension was applied to $\partial E_x/\partial y$ and $\partial E_y/\partial x$ of the following Faraday's law.

$$H_z^{n+\frac{1}{2}}\left(i+\frac{1}{2},j-\frac{1}{2},k\right)=H_z^{n-\frac{1}{2}}\left(i+\frac{1}{2},j-\frac{1}{2},k\right)-K_{3z}\left(i+\frac{1}{2},j-\frac{1}{2},k\right)$$
$$\times\left\{\frac{\partial E_y^n(i+1/2,j-1/2,k)}{\partial x}-\frac{\partial E_x^n(i+1/2,j-1/2,k)}{\partial y}\right\} \quad (16)$$

The following difference including the above mentioned truncation error of first order was used.

$$\frac{\partial E_x^n\left(i+\frac{1}{2},j-\frac{1}{2},k\right)}{\partial y}=\frac{E_x^n\left(i+\frac{1}{2},j,k\right)-E_x^n\left(i+\frac{1}{2},j-1,k\right)}{\Delta y\left(1+\frac{EK}{\Delta y}\right)}+O(1) \quad (17)$$

The derivation of (17) can be proved in the appendix A.

To make truncation error of first order into that of second order, (B-4) in the appendix B is applied to (16). Therefore, we can derive the following method to deal with a slant wire without truncation error of first order.

$$
\begin{aligned}
&H_z^{n+\frac{1}{2}}\left(i+\frac{1}{2}, j-\frac{1}{2}, k\right)=H_z^{n-\frac{1}{2}}\left(i+\frac{1}{2}, j-\frac{1}{2}, k\right)-K_{3z}\left(i+\frac{1}{2}, j-\frac{1}{2}, k\right)\\
&\times\frac{1}{\Delta x \Delta y\left(1+\frac{EK}{\Delta y}\right)}\left\{E_x^n\left(i+\frac{1}{2}, j-1, k\right)\Delta x+E_y^n\left(i+1, j-\frac{1}{2}, k\right)\left(1+\frac{EF}{\Delta y}\right)\Delta y\right.\\
&-E_y^n\left(i, j-\frac{1}{2}, k\right)\left(1+\frac{AB}{\Delta y}\right)\Delta y+\frac{EK}{2}\Delta x(\Delta y+EK)\\
&\left.\times\frac{E_x^n\left(i+\frac{1}{2}, j-1, k\right)-2E_x^n\left(i+\frac{1}{2}, j-2, k\right)+E_x^n\left(i+\frac{1}{2}, j-3, k\right)}{\Delta y^2}\right\}
\end{aligned}
\tag{18}
$$

In other words, when a slant wire can be modeled for a surge analysis, (18) is used in stead of (14). $H_x$( $i$+1/2, $j$+1/2, $k$ ) can be derived similarly.

## IV. Simulation Results and Measurements in Horizontal Conductor System

Fig. 3 shows a horizontal conductor system, which is one of the fundamental cases to learn surge propagation on a conductor. In Fig. 3, a wire with length 4 m is placed above a copper plate at height 0.6 m. The horizontal conductor is excited by a pulse generator (PG) of which the internal resistance is 50 Ω, and connected via a vertical conductor. Fig. 4 shows a source voltage wave form approximated from a measured open voltage of PG. In this configuration, voltage and current waveforms at the sending end were measured [10], and the FDTD simulations were also carried out. In the simulations where the horizontal conductor was modeled on the FDTD grids as a configuration of Fig. 3 (b), the dimensions of the analysis space were 6 m, 2 m and 2 m in the x, y and z directions respectively, and the space step was 5 cm. In the simulations where the horizontal conductor was modeled out of the FDTD grids as a configuration of Fig. 3 (c), the dimensions of the analysis space were 4 m, 4 m and 2 m in the x, y and z directions respectively, and the space step was 5 cm. All the six boundaries were treated as the second-order Liao's absorbing boundary. The resistivity of the copper plate is $1.69\times10^{-8}$ Ωm.

Fig. 5 (a), (b) and (c) show the measured and calculated waveforms of voltage at the sending end, and the calculated results were derived in cases of the wire model on grids, the simplified slant wire model and the detail slant wire model. Fig. 6 (a) shows the comparison of current at the sending end between the measured result and the calculated result in the case of the wire model on grids. Fig. 6 (b) shows the comparison between the calculated result with the wire model on grids and that with a simplified slant wire model. Fig. 6 (c) shows the comparison between the calculated result with the wire model on grids and the calculated result with the detailed slant wire model. From Fig.5, the calculated voltage waveforms with the proposed slant wire models at the sending end agree well with that with the wire model on grids. It should be noted that the wire model on grids is most accurate in FDTD simulations. The calculation results of current at the sending end in the case of the proposed slant wire models agree well with that with the wire model on grids. In Table 1, the comparisons of those propagation times and those peek values of current are shown. Table 1 shows that the proposed detailed slant wire model is more accurate than the proposed simplified one. However, the proposed simplified slant wire model is also accurate enough to be applied to lightning surge simulations.

All the calculation results of current are compensated by the following (19), (20) and (21) to take the rise time (2 ns) of CT ( Current Transformer ) into account.

$$s(t)=1-\exp\left(-\frac{t}{2\times10^{-9}}\right) \tag{19}$$

$$h(t)=\frac{\exp\left(-\frac{t}{2\times10^{-9}}\right)}{2\times10^{-9}} \tag{20}$$

$$i_0(t)=h(t)*i(t) \tag{21}$$

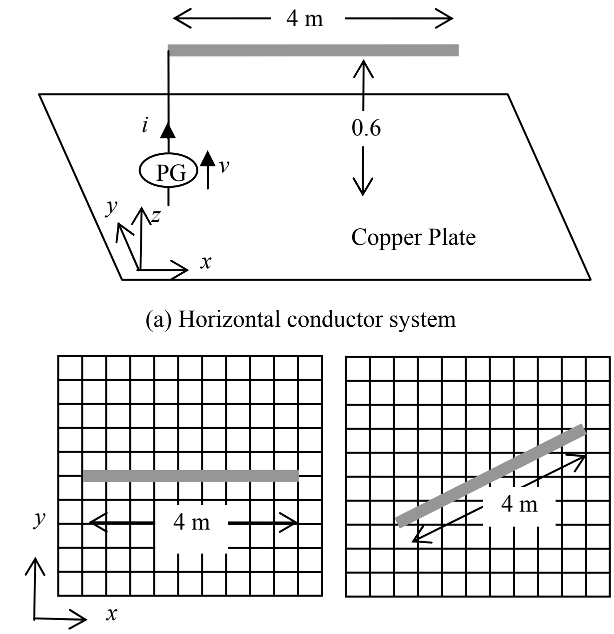


(a) Horizontal conductor system

(b) Case of the wire on FDTD grids (c) Case of the slant wire

Fig.3 Example case

Table 1 Comparisons of the propagation time and the peak value of current

| | Propagation time [ns] | Peak value of current [A] |
|---|---|---|
| Measured result | 29.39 | 0.5415 |
| Wire on FDTD grids | 28.81 | 0.5464 |
| Simplified slant wire | 29.97 (+4.03%) | 0.5150 (-5.75%) |
| Detail slant wire | 29.58 (+2.67%) | 0.5386 (-1.43%) |

* The percent expressions are comparisons on the basis of the wire model on FDTD grids

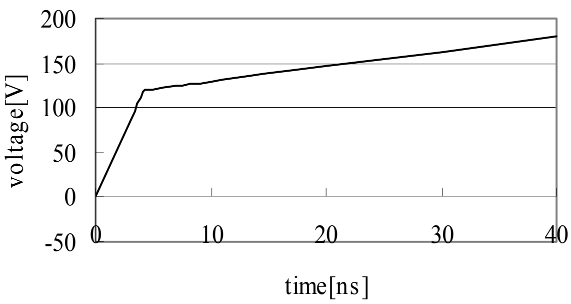


Fig. 4 PG voltage waveform

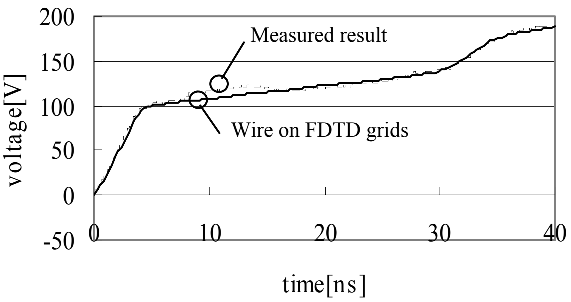


(a) Measured result and calculated result using a wire on grid

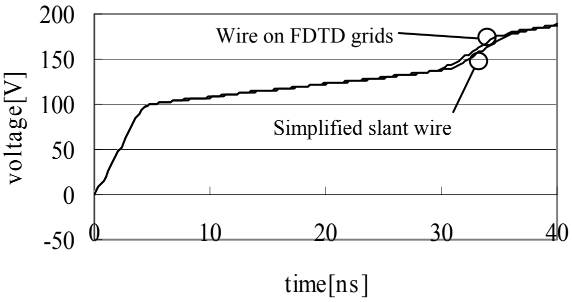


(b) Calculated result using a wire on grid and calculated result using a simplified slant wire

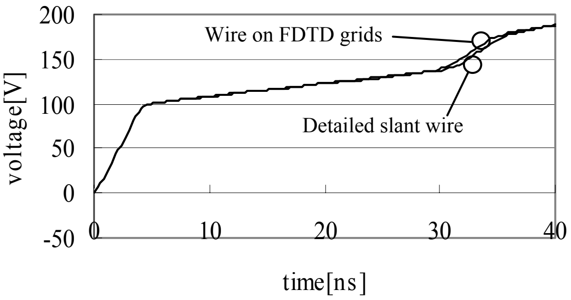


(c) Calculated result using a wire on grid and calculated result using a detail slant wire

Fig. 5 Comparison of measured and calculated results of voltage waveforms at the sending end

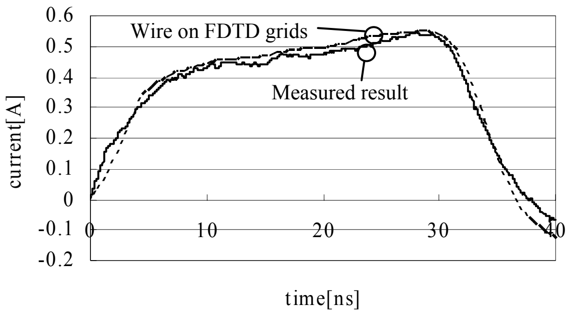


(a) Measured result and calculated result using a wire on grid

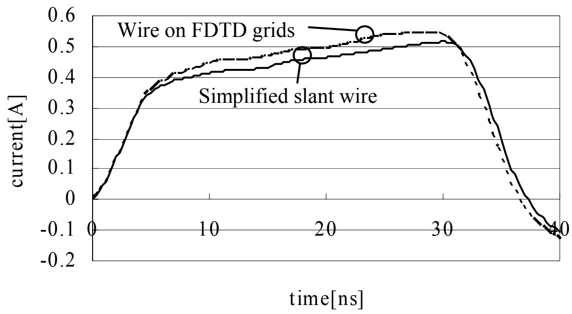


(b) Calculated result using a wire on grid and calculated result using a simplified slant wire

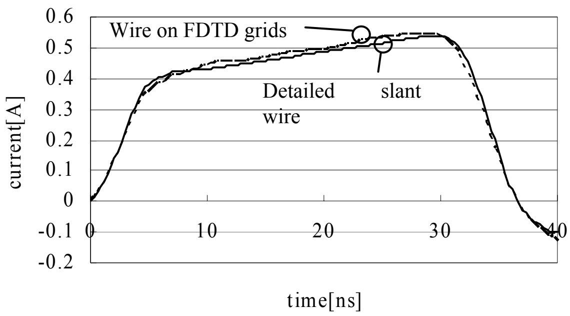


(c) Calculated result using a wire on grid and calculated result using a detail slant wire

Fig. 6 Comparison of measured and calculated results of current waveforms at the sending end

## V. Conclusions

In this paper, simplified and detail slant wire models with an accuracy correction technique to decrease error caused by the slant wires in the FDTD simulation have been proposed to generalize FDTD surge analysis programs. The comparisons with the measured result and the calculation result with a wire model on grids on a horizontal conductor system have shown to prove the accuracy of the proposed methods. As the proposed detail slant wire model adopts an implicit scheme around a slant wire, and allows for the distorted path of integration around a slant wire, error of the propagation time and the peak value of current becomes smaller than that of another slant wire. It has been shown that the simplified slant wire model is more stable than the detail model when a lot of slant wires are used in a FDTD simulated space.

The proposed methods make it possible to analyze several power systems including several physical relationships of wires in 3-Dimentions.

## VI. Appendixes

### *A. Derivation of (17)*

The following Taylor series can be shown for the derivation of (17).

$$E_x^n\left(i+\frac{1}{2},j-\frac{1}{2}-\frac{1}{2},k\right)=E_x^n\left(i+\frac{1}{2},j-\frac{1}{2},k\right) -\frac{\Delta y}{2\cdot 1!}E_x^n\left(i+\frac{1}{2},j-\frac{1}{2},k\right)'+\frac{\Delta y^2}{4\cdot 2!}E_x^n\left(i+\frac{1}{2},j-\frac{1}{2},k\right)'' -\frac{\Delta y^3}{8\cdot 3!}E_x^n\left(i+\frac{1}{2},j-\frac{1}{2},k\right)'''+\cdots \qquad \text{(A-1)}$$

$$E_x^n\left(i+\frac{1}{2},j-\frac{1}{2}+\frac{l}{2},k\right)=E_x^n\left(i+\frac{1}{2},j-\frac{1}{2},k\right) +\frac{l\Delta y}{2\cdot 1!}E_x^n\left(i+\frac{1}{2},j-\frac{1}{2},k\right)'+\frac{(l\Delta y)^2}{4\cdot 2!}E_x^n\left(i+\frac{1}{2},j-\frac{1}{2},k\right)'' +\frac{(l\Delta y)^3}{8\cdot 3!}E_x^n\left(i+\frac{1}{2},j-\frac{1}{2},k\right)'''+\cdots \qquad \text{(A-2)}$$

where: $l$ = 1+2EK/Δ$y$. From (A-1) - (A-2), the following (A-3) can be derived

$$\frac{\partial E_x^n\left(i+\frac{1}{2},j-\frac{1}{2},k\right)}{\partial y}=\frac{E_x^n\left(i+\frac{1}{2},j+\frac{EK}{\Delta y},k\right)-E_x^n\left(i+\frac{1}{2},j-1,k\right)}{(\Delta y+EK)} -\frac{EK}{2}E_x^n\left(i+\frac{1}{2},j-\frac{1}{2},k\right)''+O(2) =\frac{E_x^n\left(i+\frac{1}{2},j+\frac{EK}{\Delta y},k\right)-E_x^n\left(i+\frac{1}{2},j-1,k\right)}{(\Delta y+EK)}+\delta(EK)+O(2) \qquad \text{(A-3)}$$

where: $\delta$ is Kronecker's delta. (A-3) shows that (14) and (15) have truncation error of first order.

*B. Elimination of truncation error of first order*

The following proposed method makes truncation error of first order into that of second order. The newly defined Taylor series can be shown as:

$$E_x^n\left(i+\frac{1}{2},j-\frac{3}{2},k\right)'=E_x^n\left(i+\frac{1}{2},j-\frac{1}{2},k\right)' -\frac{\Delta y}{1}E_x^n\left(i+\frac{1}{2},j-\frac{1}{2},k\right)''+\frac{\Delta y^2}{2}E_x^n\left(i+\frac{1}{2},j-\frac{1}{2},k\right)''' -\frac{\Delta y^3}{6}E_x^n\left(i+\frac{1}{2},j-\frac{1}{2},k\right)''''+\cdots \qquad \text{(B-1)}$$

$$E_x^n\left(i+\frac{1}{2},j-\frac{5}{2},k\right)'=E_x^n\left(i+\frac{1}{2},j-\frac{1}{2},k\right)' -\frac{2\Delta y}{1}E_x^n\left(i+\frac{1}{2},j-\frac{1}{2},k\right)''+2\Delta y^2E_x^n\left(i+\frac{1}{2},j-\frac{1}{2},k\right)''' -\frac{4\Delta y^3}{3}E_x^n\left(i+\frac{1}{2},j-\frac{1}{2},k\right)''''+\cdots \qquad \text{(B-2)}$$

From (B-1) and (B-2), the following equation can be derived.

$$\frac{EK}{2}\frac{E_x^n\left(i+\frac{1}{2},j-\frac{3}{2},k\right)'-E_x^n\left(i+\frac{1}{2},j-\frac{5}{2},k\right)'}{\Delta y} =\frac{EK}{2}\left\{E_x^n\left(i+\frac{1}{2},j-\frac{1}{2},k\right)''-\frac{3\Delta y^2}{2}E_x^n\left(i+\frac{1}{2},j-\frac{1}{2},k\right)''' +\frac{7\Delta y^2}{6}E_x^n\left(i+\frac{1}{2},j-\frac{1}{2},k\right)''''+\cdots\right\} \qquad \text{(B-3)}$$

From (A-3) + (B-3),

$$\frac{\partial E_x^n\left(i+\frac{1}{2},j-\frac{1}{2},k\right)}{\partial y}=\frac{E_x^n\left(i+\frac{1}{2},j+\frac{EK}{\Delta y},k\right)-E_x^n\left(i+\frac{1}{2},j-1,k\right)}{(\Delta y+EK)} -\frac{EK}{2}\frac{E_x^n\left(i+\frac{1}{2},j-\frac{3}{2},k\right)'-E_x^n\left(i+\frac{1}{2},j-\frac{5}{2},k\right)'}{\Delta y}+O(2) =\frac{E_x^n\left(i+\frac{1}{2},j+\frac{EK}{\Delta y},k\right)-E_x^n\left(i+\frac{1}{2},j-1,k\right)}{(\Delta y+EK)} -\frac{EK}{2}\frac{E_x^n\left(i+\frac{1}{2},j-1,k\right)-2E_x^n\left(i+\frac{1}{2},j-2,k\right)+E_x^n\left(i+\frac{1}{2},j-3,k\right)}{\Delta y^2}+O(2) \qquad \text{(B-4)}$$

From the comparison between (A-3) and (B-4), the truncation error of first order in (A-3) can be eliminated in (B-4).

## REFERENCES


[1] W. Scott-Meyer, EMTP Rule Book, B.P.A.,1984.

[2] K. S. Yee, "Numerical solution of initial boundary value problems involving Maxwell's equations in isotropic media ", IEEE Trans., Antennas & Propag., Vol.. AP-14, No. 3, pp. 302-307, 1966.

[3] K. S. Kunz and R. J. Luebbers, *The Finite Difference Time Domain Method for Electromagnetics*, Boca Raton, FL:CRC, 1993.

[4] T. Namiki, K. Ito, "A proposal of accuracy correction technique in FDTD method when nonuniform Cells are used", Technical Report of IEICE, pp55-60, 2001.

[5] K. Tanabe, "A Method for Computational Analysis of Transient Resistance for Grounding Systems Based on the FD-TD Method", Trans. of IEEJ, Vol.120-B, No. 8/9, pp1119-1125, 2000.

[6] N. Tanabe, et al., "A Transient Analysis of a Cable with a Two-Layer Conductor by FDTD Method", Trans. of IEEJ, Vol.121-B, No. 11, pp1566-1571, 2001.

[7] J. Fang, J. Ren, "A Locally Conformed Finite- Difference Time Domain Algorithm of Modeling Arbitrary Shape Planar Metal Strips ", IEEE Trans., Microwave Theory Tech., Vol. 41, pp. 830-838, Apr. 1993.

[8] K. S. Yee, J. S. Chen and A. H. Chang, "Conformal Finite-Difference Time-Domain (FDTD) with Overlapping Grids", IEEE Trans., Antennas & Propag., Vol. 40, pp. 1068-1075, 1992.

[9] N. Tanabe, "Modeling of Arbitrary-Shaped Conductors for Electromagnetic Field Analysis with FDTD Method", Master Thesis in Doshisha Univ. in Japan, 2001.

[10]T. Noda, "Thin Wire Representation in Finite Difference Time Domain Surge Simulation", IEEE Trans., Power Delivery, Vol. 17, No. 3, July 2002.

[11]K. Yamamoto, H. Iki, "A Diagonal Wire in an Electromagnetic Analysis Based on the Finite-Difference Time-Domain Method", Proceedings of 13th Annual Conference of Power & Energy Society, IEE of Japan, Vol. A, pp.234-239, 2002.


## ACKNOWLEDGMENTS

The authors would like to express their gratitude to Prof. A. Ametani and Dr. Y. Baba (Doshisha University, Kyoto, Japan) for their instructive advises for our researches.